Am J Transl Res 2024;16(11):7186-7199
www.ajtr.org /ISSN:1943-8141/AJTR0159997

Original Article

Twelve Shugan Lidan Granules from traditional Chinese medicine can improve liver function in patients with postoperative hepatolithiasis by inhibiting the Hippo signaling pathway

Lixiang Li[1,2,4*], Xiaoyong Niu[1,5*], Wanzong Zhang[1,4*], Ziyu Wang[3], Shengming Zhang[1,4], Qi Zhang[1,4], Wei Qi[1,4], Wenshan Jing[1,4], Gaobin Hu[1,4], Long Huang[1,4], Ziyi Li[1,4], Qiyu Feng[3], Hui Peng[1,4], Qingsheng Yu[1,4]

[1]Department of General Surgery, The First Affiliated Hospital of Anhui University of Chinese Medicine, Hefei 230031, Anhui, P. R. China; [2]Department of General Surgery, The People's Hospital of Lujiang County, No. 32, Wenming Middle Road, Lujiang County, Hefei 230036, Anhui, P. R. China; [3]Cancer Research Center, The First Affiliated Hospital of USTC, Division of Life Sciences and Medicine, University of Science and Technology of China, Hefei 230036, Anhui, P. R. China; [4]Institute of Chinese Medicine Surgery, Anhui Academy of Chinese Medicine, Hefei 230031, Anhui, P. R. China; [5]The First Clinical Medical College of Anhui University of Chinese Medicine, Hefei 230031, Anhui, P. R. China. [*]Equal contributors.

Received August 22, 2024; Accepted November 19, 2024; Epub November 25, 2024; Published November 30, 2024

Abstract: Introduction: Hepatolithiasis (HL) is a complex liver and biliary disorder characterized by high rates of recurrence. This study aimed to evaluate the efficacy of Twelve Shugan Lidan Granules (TSLG), a compound herbal traditional Chinese formulation, in the treatment of HL, as well as to investigate its underlying mechanism. Methods: A retrospective analysis was conducted involving 157 patients diagnosed with HL, who were divided into two groups: the control group and the research group. In the control group, no treatment was given postoperatively, while in the research group, TSLG was orally administered three times a day postoperatively for two months. Both groups were followed up by telephone at 1 month, 2 months, and 3 months postoperatively. Liver function indicators were measured before and after surgery, and miRNA expression profiling was analyzed using high-throughput sequencing (HTS). Additionally, the expression levels of related proteins were assessed through western blots. Results: Postoperative liver function indicators were significantly lower in the research group compared to the control group ($P < 0.05$). Additionally, 64 miRNAs were differentially expressed in HL patients. Further analysis of 64 miRNAs revealed their abnormal targeting of the Hippo signaling pathway. Further experimental results indicate that TAZ protein expression is elevated in HL patients, reflecting abnormal activation of the Hippo signaling pathway in these patients. TSLG treatment significantly reduced the expression of YAP, TAZ, and SREBP-2 proteins, while increasing the expression of p-YAP and p-TAZ proteins (all $P < 0.05$). Furthermore, TSLG inhibited the Extracellular Acidification Rate (ECAR) in LPS-induced WRL68 cells. Conclusion: TSLG effectively improved postoperative liver function by downregulating sterol regulatory element-binding protein-2 (SREBP-2) and inhibiting the Hippo signaling pathway.

Keywords: Hepatolithiasis, Twelve Shugan Lidan Granules, Hippo signaling pathway, cholesterol metabolism, miRNAs

Introduction

Hepatolithiasis (HL), also known as intrahepatic calculi, is a condition characterized by the formation of stones within the intrahepatic bile ducts, which are located beyond the bifurcation of the right and left hepatic ducts [1-5]. This disease is more prevalent in Southeast and East Asian countries but remains relatively uncommon in western nations [2, 3, 5, 6]. However, with increasing immigration from Asia, hepatolithiasis has emerged as a clinical challenge in western countries [2, 3, 5, 6]. The incidence of hepatolithiasis varies significantly across China, with higher occurrence rates primarily observed in North China, Southwest China, South China, and the Yangtze River Basin region [3, 7, 8].

Most biliary stones associated with hepatolithiasis are soft and prone to fragmentation, com-

https://doi.org/10.62347/VXHU6738

monly referred to as brown pigment stones or calcium bilirubinate stones. These stones consist of a complex mixture of cholesterol and cholesterol-based components, indicating a complicated pathogenesis that involves both calcium bilirubinate deposition and cholesterol solubility [9]. Several key factors contributing to pathogenic changes in the hepatobiliary system that facilitate stone formation have been identified. These factors include disorders of bile metabolism, infections, bile duct injury, and cholestasis [1-3, 10, 11]. However, the precise pathogenesis of hepatolithiasis remains incompletely understood.

Hepatolithiasis presents a significant challenge for patients due to its high recurrence rate and the necessity for repeated surgical intervention, including hepatectomy, endoscopic lithotomy, and lithotripsy [4-6, 12-16]. This highlights the urgent need for effective treatment options, since failure to address the condition promptly and appropriately may result in serious complications, including intrahepatic cholangiocarcinoma [17, 18]. The optimal treatment strategy for hepatolithiasis depends on individual patient characteristics, and various therapies have been developed in recent years, including pharmacologic treatments, endoscopic lithotomy, and other surgical interventions [12-16, 19].

Traditional Chinese medicine has also been utilized in the treatment of hepatobiliary diseases, including hepatolithiasis. The in-hospital preparation from our institution, Twelve Shugan Lidan Granules (TSLG), is a traditional Chinese herbal medicine used to enhance hepatobiliary and enteric function. It is employed as an empirical prescription for the clinical treatment of postoperative recurrence of intrahepatic bile duct stones at our hospital [18-21]. TSLG comprises several key ingredients: Bupleurum, Curcuma aromatica, Fructus aurantii immaturus, Magnolia officinalis, raw rhubarb, Scutellaria baicalensis, red peony root, Herba Lysimachiae, plantain, Folium Pyrrosiae, Salvia miltiorrhiza, and white peony root [22]. Among these, *Radix bupleuri* has been reported to promote hepatic function [23-25], which is able to prevent stone formation. Additionally, *Turmeric supplementation* can also improve liver function both in patients and animals [26-28]. Moreover, *Radix paeoniae* is found to protect against hepatic damage [29-31]. Several ingredients of TSLG have also shown hepatoprotective effects when extracted from their respective components.

For instance, dihydrotanshinone I, a natural monomeric compound isolated from Salvia miltiorrhiza, has been shown to improve liver function and mitigate liver fibrosis [32]. The results of the mass spectrometry analysis for each component are presented in Annex 1. These liver protective effects may provide a foundation for the therapeutic efficacy of TSLG in in the treatment of hepatolithiasis. Therefore, in this study, we investigated the clinical efficacy of Twelve Shugan Lidan Granules (TSLG) in treating hepatolithiasis and its underlying mechanism.

Methods

Clinical efficacy of Twelve Shugan Lidan Granules

Data sources: Retrospective analysis of patients admitted to the Department of General Surgery of Anhui Hospital of Traditional Chinese Medicine from January 2021 to December 2022, Sample size estimation was based on previous observations of clinical efficacy by our team. The study design is illustrated in **Figure 1**. Ethical approval number for this study: 2022AH-41.

Inclusion criteria: Diagnosis of hepatolithiasis by color ultrasound, CT, or MRCP followed by surgical treatment. Post-treatment confirmation of no residual stones by CT, MRCP, cholangiography or other imaging examinations.

Exclusion criteria: Patients with lower common bile duct stenosis and sphincter of the duodenal papilla insufficiency. Patients with concurrent hepatobiliary malignancy. Patients with other organ dysfunctions that make them unable to tolerate surgery.

Details of study interventions

Both groups underwent surgery performed by the same team of surgeons. Laparoscopic common bile duct exploration with T-tube drainage was conducted as follows: a pneumoperitoneum was established using the four-port method, allowing visualization of the common bile

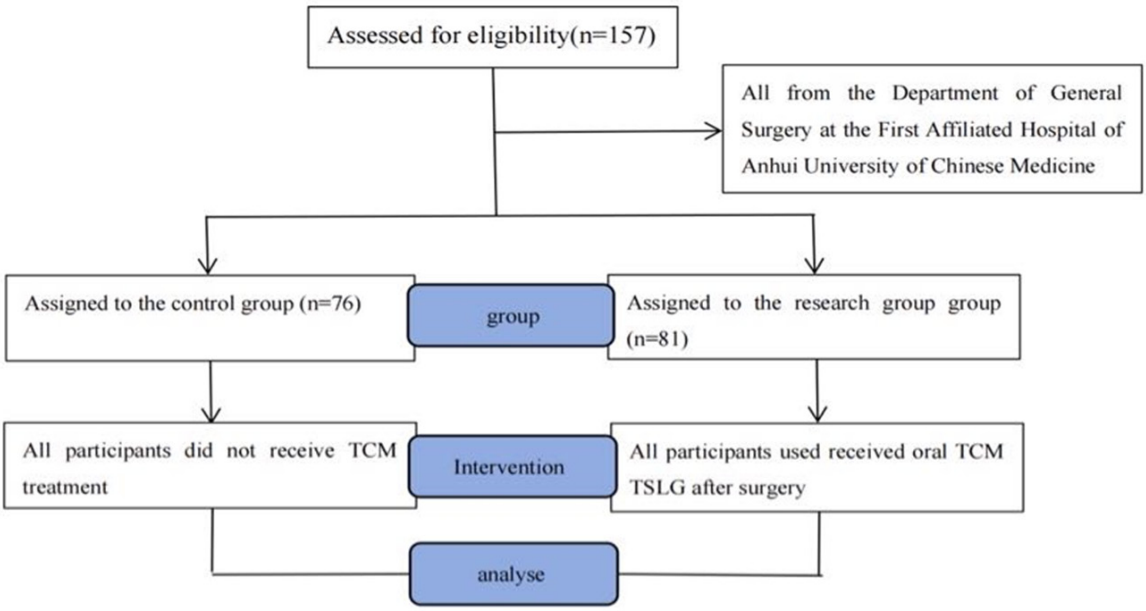

Figure 1. Flow chart for patient assignment.

duct, cystic duct, and left and right hepatic ducts. Bile was extracted from the common bile duct puncture site, followed by vertical dissection of the common bile duct. A choledochoscope was then inserted to locate the stones, which were subsequently removed using a net basket. After confirming that no residual stones remained, a T-tube was placed, and absorbable sutures were used to close the anterior wall of the common bile duct. Postoperative treatment included antibiotics, nutritional support, liver protection, and other supportive measures. After surgery, patients in the research group received TSLG orally. On the second day post-surgery, patients began taking Twelve Shugan Lidan Granules (Anhui Medicine Z20080011, prepared by the Preparation Center of the First Affiliated Hospital of Anhui University of Traditional Chinese Medicine). Each dose consisted of one bag (6 g) dissolved in 100 ml of warm water, administered orally three times a day. The duration of treatment was determined by subsequent ultrasound and MRCP examinations for stones, continuing until the stones were cleared and liver function returned to normal levels.

Observation indicators and methods

The diameters and numbers of stones of patients in the two groups were collected. Stone properties: FTIR spectroscopy (Bruker ALPHA II) was used to analyze the stone composition and record the data. Liver function indicators were assessed by extracting 5 ml of venous blood at 7:00 a.m. on the 1st, 3rd, and 7th days post-surgery. The blood samples were processed using an automatic biochemical analyzer (Hitachi 7600-020) and analyzed using the circulating enzyme rate method. The levels of alanine aminotransferase (ALT), aspartate aminotransferase (AST), total bilirubin (TB), and albumin (ALB) were measured and recorded.

Tissue samples

Hepatic biopsies were obtained from five patients diagnosed with hepatolithiasis and five patients with hepatic hemangioma (HH) from the Department of General Surgery at the First Affiliated Hospital of Anhui University of Chinese Medicine, with informed consent from all participants. The liver biopsies from the hepatolithiasis patients were designated as the HL group, while those from the HH patients were designated as the normal group (NOR), as their hepatobiliary function is nearly normal and they do not exhibit stone formation.

RNA extraction and sequencing

Total RNA was isolated from each hepatic sample using TRIzol (Thermo Fisher Scientific, USA) and the RNeasy Mini Kit (Qiagen, Germany).

The quantity and quality of the RNA were assessed using a Qubit 4.0 Fluorometer (Thermo Fisher Scientific, USA), while RNA integrity was evaluated through agarose gel electrophoresis.

The miRNA library was prepared using the Illumina TruSeq Stranded Total RNA Sample Preparation Kits (Illumina, San Diego, CA) with approximately 1 μg of total RNA. Subsequent quantification was performed using a Qubit 4.0 Fluorometer (Thermo Fisher Scientific, USA). Additionally, reverse transcription-polymerase chain reaction (RT-PCR) was conducted to create clusters, and the target band of 145-160 bp was recovered by PAGE electrophoresis. The clusters were then sequenced on the Illumina HiSeq (Illumina, USA). All sequencing was performed by Genergy Biotechnology Inc. (Shanghai, China).

Prediction of conserved and novel miRNAs

The Fastx-Toolkit software (Version 0.0.14, http://hannonlab.cshl.edu/fastx_toolkit/) was employed to remove splice sequences and low-quality fragments from the 3' end of the sequencing data. Sequences containing 14-40 nucleotides were selected for downstream analysis. Bowtie software (Version 1.2.2) was used to map the miRNAs against the reference genome, Rfam sequence database, RepBase sequence database, and miRBase sequence database. Novel miRNAs were predicted using miRDeep 2 software (Version 2.0.0.5), while conserved miRNAs were identified by searching miRBase (http://www.mirbase.org/).

Differential expression analysis of miRNAs

The differential expression of miRNAs between the HL and NOR groups was analyzed using DESeq2 software (Version 1.22.1), with counts per million (CPM) serving as the measurement index. A difference between the two groups was considered significant when the *p*-value was ≤ 0.05 and the $\log_2$ (fold change) was ≥ 1.

Target gene prediction and functional analysis

The target genes of the differentially expressed miRNAs were predicted using miRanda software (Version 3.3a). Gene Ontology (GO) analysis was performed for the functional annotation and classification of the target genes using TopGO software (http://www.bioconductor.org/packages/release/bioc/html/topGO.html). [54]Kyoto Encyclopedia of Genes and Genomes (KEGG) analysis was conducted to analyze the involved pathways. The significance of GO terms and pathways was determined using Fisher's exact test, with the *P*-value corrected by the Benjamini-Hochberg method to calculate the false discovery rate (FDR). Only GO terms and pathways with a corrected *P*-value < 0.05 were selected for further analysis.

Western blot

We prepared liver tissue or cells for western blots. NP40 and 1% PMSF (American Abcam Company) were used as protease inhibitors for the extraction of total protein samples, followed by a facility fee of 15,000 centrifugation for 10 minutes. 20 μg protein samples were separated by 5% concentrated gel and 10% separated gel in the electrophoresis apparatus (Bio Rad Company), and then transferred to 0.45 μm NC membrane using the membrane converter (Bio Rad Company). The membrane was blocked in TBS/Tween-20 containing 5% skimmed milk powder for 1 hour, after which the primary antibody was incubated overnight at 4°C. Following the incubation with the secondary antibody, visual detection was performed. The antibodies used for immunoblots included GAPDH (ab263962), SREBP-2 (ab30682), phospho-YAP (ab76252), and TAZ (ab119373) from Abcam, as well as YAP (No. 14074) and phospho-TAZ (No. 75275) from Cell Signaling Technology. The expression of GAPDH was used as the reference band.

Cell culture

LX-2 human hepatic stellate cells, MHCC97-H human metastatic HCC cells, and WRL68 human hepatic cells (abbreviated as LX-2, 97H, and WRL68, respectively) were purchased from the Shanghai Institute of Cell Science, China. These cell lines were cultured in flasks containing Dulbecco's Modified Eagle's Minimal Essential Medium (DMEM), supplemented with 10% (v/v) fetal bovine serum, 100 IU/mL penicillin, and 100 mg/mL streptomycin (purchased from Israel Biological Industries Company and Gibco Corporation, USA). These cells were cultured in a 5% carbon dioxide incubator maintained at 37°C (Abcam) to simulate physiologic conditions.

Selection of drug concentration

To investigate whether the efficacy of TSLG in treating HL is based on the regulation of the abnormally activated Hippo signaling pathway, we conducted cell line studies. Based on prior research conducted by our group, TSLG was dissolved in DMEM at a concentration of 100 mg/mL, creating concentration gradients of 0, 1.25, 2, 2.5, and 5 mg/mL. LX-2, WRL68, and MHCC97-H cells were treated with TSLG. After 48 hours, CCK-8 reagent (purchased from Gibco, USA) was added to the cultured cells, and the reading at 450OD was detected using an enzyme-linked immunosorbent assay (ELISA) reader. The cell proliferation was determined based on the reading results to determine the optimal drug concentration.

Drug intervention and western blot

TGFβ-1[41] (5 ng/mL) (purchased from R&D Systems, USA) was added to LX-2 cells to activate the Hippo signaling pathway, resulting in the upregulation of YAP and TAZ and the downregulation of p-YAP and p-TAZ. Subsequently, traditional Chinese medicine TSLG was added for intervention. For MHCC97-H and WRL68 cells, the drug intervention was performed directly. Forty-eight hours later, cell lysates were collected, and protein expression was analyzed by western blot.

Seahorse XF analysis

To investigate the impact of TSLG intervention on glucose metabolism in WRL68 cells, the extracellular acidification rate (ECAR) was measured using Seahorse XF glycolysis stress tests. TSLG was dissolved in DMEM at a concentration of 100 mg/mL, and an optimal concentration was selected. WRL68 cells were induced with LPS[42] (100 ug/mL) (Purchased from R&D Systems, USA) for 6 hours, followed by treatment with TSLG. Glucose metabolism was evaluated after 24 hours. GraphPad Prism 9.0 software was utilized to measure ECAR as an assessment of key measures of glycolytic flux.

Statistical methods

Statistical analysis was performed using SPSS 21.0 software. Measured data were expressed as mean ± standard deviation (SD). An independent samples t-test was used for comparisons between two independent samples, while repeated measured data were analyzed using repeated measures analysis of variance. Counted data were presented as counts or percentages, and the χ^2 test was used for comparisons. A *p*-value of less than 0.05 was considered significant.

Results

Clinical efficacy of Twelve Shugan Lidan Granules in treating hepatolithiasis

As shown in **Table 1**, there were no significant differences in the general conditions of the two groups. However, after surgery, significant differences were observed in the levels of ALT (F = 10.35, P = 0.002), AST (F = 15.71, P = 0.001), TB (F = 27.62, P = 0.001), and TBA (F = 4.72, P = 0.031) between the two groups. Notably, ALT and TBA levels increased on the third day after surgery and decreased by the seventh day. In contrast, AST and TB levels declined over time following surgery. There were no significant differences in ALT, AST, TB, and TBA levels between the two groups one day before surgery (all $P > 0.05$). On the third and seventh days postoperatively, ALT, AST, TB, and TBA levels in the control group were significantly higher than those in the TSLG group (all $P < 0.05$). Additionally, there were no significant differences in preoperative and postoperative ALB levels between the two groups (all $P > 0.05$), as shown in **Table 2**. These results indicate that liver function in the TSLG group was significantly improved compared to the control group, suggesting a favorable therapeutic effect. This improvement may be attributed to a deceleration of bilification, which may help prevent stone recurrence.

Differentially expressed miRNAs and abnormal activation of Hippo signaling pathway in HL patients

We compared the miRNA expression profiles between the HL group (hepatolithiasis) and the NOR group (hepatic hemangioma). As shown in **Figure 2A**, the volcano plot displays all detected miRNAs, while **Figure 2B** presents the heatmap of cluster analysis, illustrating significant differences in miRNA expression patterns between the two groups. A total of 64 miRNAs (10 novel miRNAs and 54 conserved

Table 1. Comparison of general conditions between two groups

Project	Control group (n = 76)	TLSG group (n = 81)	Statistics	*P* value
Gender [n (%)]				
Male	37 (48.68%)	41 (50.62%)		
Female	39 (51.32%)	40 (49.38%)	0.058	0.80
Age (years)	60.85±15.91	59.55±16.26	0.50	0.61
BMI	24.59±5.91	23.90±5.88	0.72	0.46
Basic disease [n (%)]				
Viral hepatitis	9 (11.84%)	11 (13.58%)	0.10	0.74
Fatty liver	15 (19.74%)	20 (24.69%)	3.84	0.45
The number of gallstones [n (%)]				
1	10 (13.16%)	15 (18.52%)		
≥ 2	66 (86.84%)	66 (81.48%)	0.84	0.35
The gallstone diameter				
≥ 10 mm	36 (47.37%)	42 (51.85%)		
< 10 mm	40 (52.63%)	39 (48.15%)	0.31	0.57
Properties of gallstone [n (%)]				
Pigmental stones	48 (63.16%)	55 (67.90%)		
Mixed stones	28 (36.84%)	26 (32.10%)	0.40	0.52

miRNAs) were identified as differentially expressed. Among these, 40 miRNAs were up-regulated and 24 miRNAs were down-regulated. The detailed results of the top 20 up-regulated and down-regulated miRNAs are shown in **Table 3** (see Annex 2 for details). To explore possible mechanisms of HL based on these differentially expressed miRNAs, we conducted GO and KEGG analyses on the target genes to evaluate possible signaling pathways and related functions. A total of 1,458 GO terms underwent enrichment and were categorized into three main GO categories: biological processes (BP), cellular components (CC), and molecular functions (MF). As illustrated in **Figure 2C**, the top ten GO terms in BP, CC, and MF were highlighted. Notably, the biological processes primarily involved were nervous system development (GO: 0007399), neuron differentiation (GO: 0030182), and neurogenesis (GO: 0022008). In the cellular component category, synapse (GO: 0045202), neuron projection (GO: 0043005), and neuron part (GO: 0097458) were the most prominent.

Notably, KEGG analysis indicated that the target genes were significantly enriched in several signaling pathways possibly related to the occurrence of hepatolithiasis (HL). As shown in **Figure 2D**, the top 20 involved signaling pathways include the Cholinergic synapse pathway (hsa04725), Hippo signaling pathway (hsa04390), Gastric cancer pathway (hsa05226), Axon guidance pathway (hsa04360), Signaling pathways regulating pluripotency of stem cells (hsa04550), and Hepatocellular carcinoma pathway (hsa05225). In particular, Hippo signaling pathway has been reported to be related to fibrosis formation [37, 38], which is also well recognized as playing a critical role in controlling organ size by regulating cell proliferation, apoptosis, and the self-renewal of stem cells [39, 40].

GO and KEGG analyses revealed the abnormal activation of the Hippo signaling pathway in hepatolithiasis (HL) patients, which may contribute to the pathogenesis of intrahepatic bile duct calculi formation. As shown in **Figure 3A**, we conducted western blot analysis of liver samples from the HL and NOR groups. **Figure 3B** and **3C** demonstrate that the expression of p-TAZ is significantly down-regulated in the HL group compared to the NOR group, while the expression of SREBP2 is markedly up-regulated in the HL group. The elevated levels of SREBP2 in the HL group suggest that the Hippo signaling pathway is indeed abnormally activated, aligning with our omics analysis.

Table 2. Comparison of changes in liver function between the two groups

Groups	Control group (n = 76)	TSLG group (n = 81)	P^N
ALT			
Preoperative 1 day	88.93±17.94	89.59±17.20	0.815
3 days after operation	135.68±68.02$^\Delta$	103.15±57.40$^\Delta$	≤ 0.001
7 days after operation	52.96±22.17$^\Delta$	44.24±22.22$^\Delta$	≤ 0.001
F^M	P^M	10.35	0.002
AST			
Preoperative 1 day	99.18±67.78	95.61±56.93	0.800
3 days after operation	68.65±28.87$^\Delta$	52.46±27.71$^\Delta$	≤ 0.001
7 days after operation	38.98±17.46$^\Delta$	35.63±17.01$^\Delta$	≤ 0.001
F^M	P^M	15.71	≤ 0.001
TB			
Preoperative 1 day	32.73±13.20	30.10±14.12	0.230
3 days after operation	40.86±14.42$^\Delta$	27.80±10.84$^\Delta$	≤ 0.001
7 days after operation	24.59±10.55$^\Delta$	18.75±7.65$^\Delta$	≤ 0.001
F^M	P^M	27.62	≤ 0.001
ALB			
Preoperative 1 day	36.40±5.32	36.70±5.13	0.537
3 days after operation	35.36±4.42	36.40±5.32	0.186
7 days after operation	37.95±4.93	39.35±4.01	0.051
F^M	P^M	3.50	0.063
TBA			
Preoperative 1 day	20.54±11.38	20.98±9.28	0.791
3 days after operation	33.18±20.76	27.90±13.01	0.056
7 days after operation	16.23±5.90	11.82±6.55	≤ 0.001
F^M	P^M	4.72	0.031

Note: 1. P^N indicates the difference between the research group and the control group at each time point when the treatment time of *in vivo* effect in the group × the group; 2. F^M, P^M refer to the difference between the research group and the control group at each time point when the treatment time of *in vivo* effect between the group × the group; 3. Compared with preoperative 1 d, $^\Delta P < 0.05$; 4. ALT, alanine aminotransferase; AST, aspartate aminotransferase; TB, total bilirubin; ALB, albumin; TBA, total bile acids.

Down-regulation of SREBP2 and suppression of Hippo signaling pathway intervened by TSLG

After intervention with TSLG at various concentrations, the CCK-8 values were measured 48 hours later. As shown in **Figure 4**, the optimal drug concentration for cell line studies in LX-2, MHCC97-H, and WRL68 cells was determined to be 1.25 mg/mL. The results from the cell line studies, illustrated in **Figure 5**, show the protein expression levels of YAP, p-YAP, TAZ, p-TAZ, SREBP2, and GAPDH following the treatment with TGFβ-1 and TSLG in different cell lines. The findings indicated that TSLG treatment led to a down-regulation of YAP and TAZ proteins, an up-regulation of p-YAP and p-TAZ proteins, and a down-regulation of SREBP2 in LX-2, MHCC97-H, and WRL68 cells. This suggests that TSLG may suppress the Hippo signaling pathway and inhibit the expression of SREBP2. Therefore, we speculate that TSLG may prevent the formation of intrahepatic bile duct calculi by inhibiting the Hippo signaling pathway.

LPS induced glycolysis and glycolysis capacity are inhibited after TSLG intervention

Seahorse XF technology was used to detect glycolysis and glycolytic capacity in WRL68 cells after LPS induction and TSLG intervention. The cells were incubated in a glycolysis stress test solution without glucose and pyruvate, and the extracellular acidification rate (ECAR) was measured to assess the relative glycolytic function of live cells following LPS and TSLG treatment. Key measures for a comprehensive evaluation of the glycolytic pathway were obtained, including glycolysis and glycolytic capacity. The experimental results indicated that LPS induction significantly increased glycolysis and glycolytic capacity in WRL68 cells. However, following TSLG intervention, both glycolysis and glycolytic capacity were significantly reduced compared to the LPS induction group, though they did not return to baseline levels. These results are shown in **Figure 6**.

Discussion

The precise pathogenesis of hepatic bile duct stones remains elusive and may involve various factors, including cholestasis, bile duct stenosis, infections, disorders of bile metabolism, and genetic mutations. The obstruction of small bile ducts caused by these stones can lead to bile duct inflammation, stenosis, and liver fibrosis, which may result in liver atrophy or cirrhosis [33, 34]. These complications can

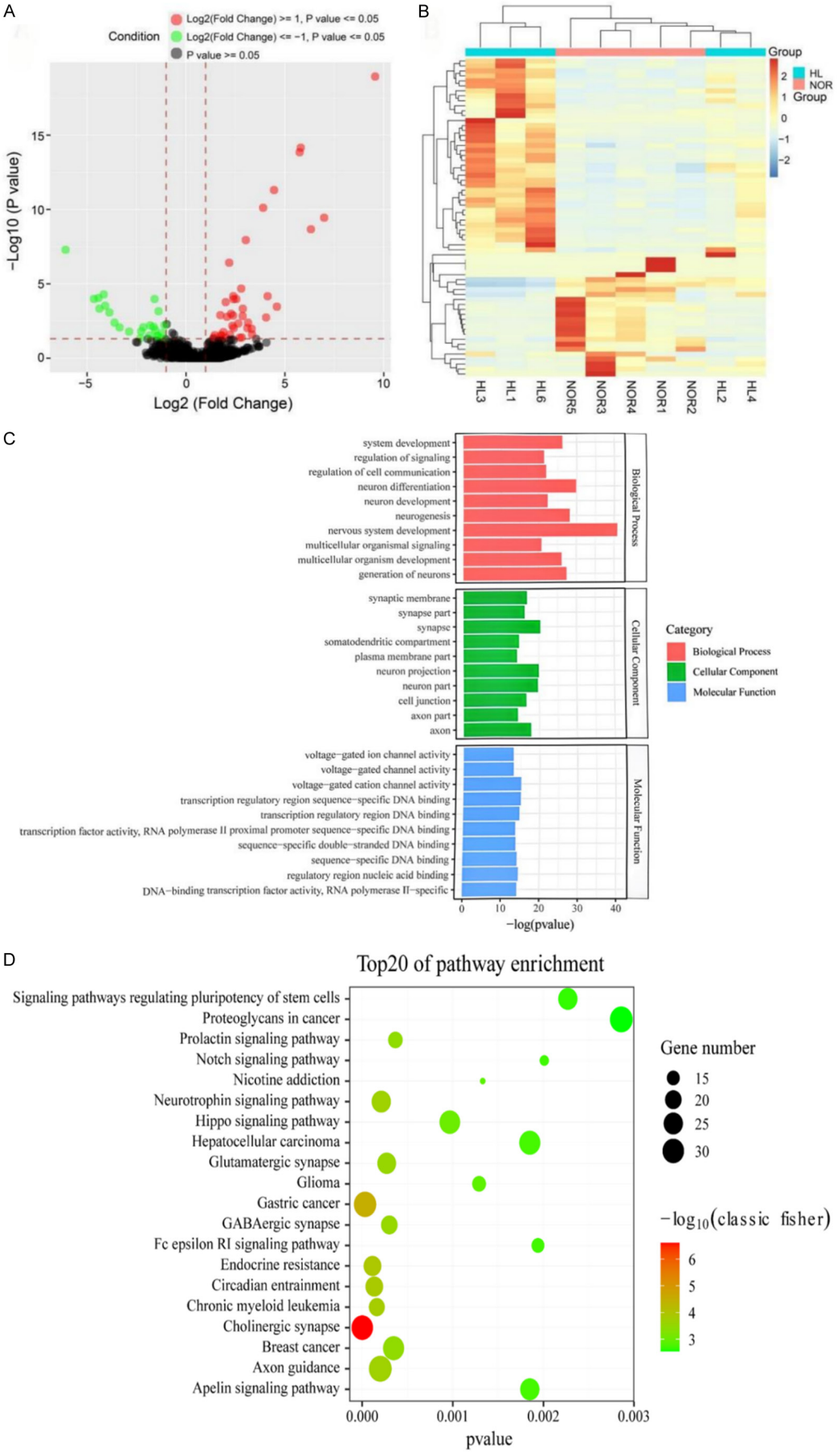
A
Log2(Fold Change) >= 1, P value <= 0.05
Condition
Log2(Fold Change) <= −1, P value <= 0.05
P value >= 0.05
−Log10 (P value)
Log2 (Fold Change)
B
Group
HL
NOR
Group
HL3
HL1
HL6
NOR5
NOR3
NOR4
NOR1
NOR2
HL2
HL4
C
system development
regulation of signaling
regulation of cell communication
neuron differentiation
neuron development
neurogenesis
nervous system development
multicellular organismal signaling
multicellular organism development
generation of neurons
Biological Process
synaptic membrane
synapse part
synapse
somatodendritic compartment
plasma membrane part
neuron projection
neuron part
cell junction
axon part
axon
Cellular Component
voltage−gated ion channel activity
voltage−gated channel activity
voltage−gated cation channel activity
transcription regulatory region sequence−specific DNA binding
transcription regulatory region DNA binding
transcription factor activity, RNA polymerase II proximal promoter sequence−specific DNA binding
sequence−specific double−stranded DNA binding
sequence−specific DNA binding
regulatory region nucleic acid binding
DNA−binding transcription factor activity, RNA polymerase II−specific
Molecular Function
−log(pvalue)
Category
Biological Process
Cellular Component
Molecular Function
D
Top20 of pathway enrichment
Signaling pathways regulating pluripotency of stem cells
Proteoglycans in cancer
Prolactin signaling pathway
Notch signaling pathway
Nicotine addiction
Neurotrophin signaling pathway
Hippo signaling pathway
Hepatocellular carcinoma
Glutamatergic synapse
Glioma
Gastric cancer
GABAergic synapse
Fc epsilon RI signaling pathway
Endocrine resistance
Circadian entrainment
Chronic myeloid leukemia
Cholinergic synapse
Breast cancer
Axon guidance
Apelin signaling pathway
pvalue
Gene number
−log10(classic fisher)

Figure 2. The miRNAs expression profiling of the two groups. A. Volcano of all detected miRNAs. B. Hierarchical clustering of differentially expressed miRNAs. HL, hepatolithiasis patient group; NOR, normal group. C. GO classification of differential expression genes in the liver tissue of HLD and NOR. D. Top 20 signaling pathways predicted to be regulated by differentially expressed genes. GO, Gene Ontology; KEGG, Kyoto Encyclopedia of Genes and Genomes; BP, biological processes; CC, cellular components; MF, molecular functions.

Table 3. Top 20 differentially expressed miRNAs between the HL group and the NOR group

miRNA	Log2FC	Type of regulation	miRNA	Log2FC	Type of regulation
hsa-miR-100-5p	2.797269941	Up	hsa-miR-106a-3p	-1.432959407	Down
hsa-miR-10b-5p	2.875506356	Up	hsa-miR-122-5p	-1.585796479	Down
hsa-miR-125b-1-3p	4.055534677	Up	hsa-miR-1307-5p	-2.309855263	Down
hsa-miR-132-3p	2.652076697	Up	hsa-miR-378a-5p	-1.557662644	Down
hsa-miR-135b-5p	4.599912842	Up	hsa-miR-4488	-3.609415544	Down
hsa-miR-141-3p	5.807977068	Up	hsa-miR-4497	-4.156749613	Down
hsa-miR-155-5p	3.906377546	Up	hsa-miR-4508	-3.355808988	Down
hsa-miR-181a-5p	2.8670737	Up	hsa-miR-4516	-3.86941589	Down
hsa-miR-181b-5p	3.145548071	Up	hsa-miR-4686	-2.155278225	Down
hsa-miR-199b-5p	4.457554438	Up	hsa-miR-4707-5p	-1.432959407	Down
hsa-miR-200c-3p	5.751097681	Up	hsa-miR-483-5p	-1.634350528	Down
hsa-miR-20b-5p	2.725650281	Up	hsa-miR-7641	-4.373458396	Down
hsa-miR-223-3p	3.10820275	Up	hsa-miR-7704	-2.872125177	Down
hsa-miR-23a-3p	2.827084392	Up	hsa-miR-885-3p	-1.846194664	Down
hsa-miR-342-3p	3.029913409	Up	Nov_10_17372	-6.081664997	Down
hsa-miR-451a	3.029913409	Up	Nov_10_17632	-1.807354922	Down
hsa-miR-708-5p	6.32089723	Up	Nov_10_17639	-4.422064766	Down
Nov_1_300	9.570045424	Up	Nov_3_6560	-4.077242999	Down
Nov_6_11375	6.991303801	Up	Nov_8_15029	-4.654310547	Down
Nov_7_12460	3.346802764	Up	Nov_9_15656	-2.263034406	Down

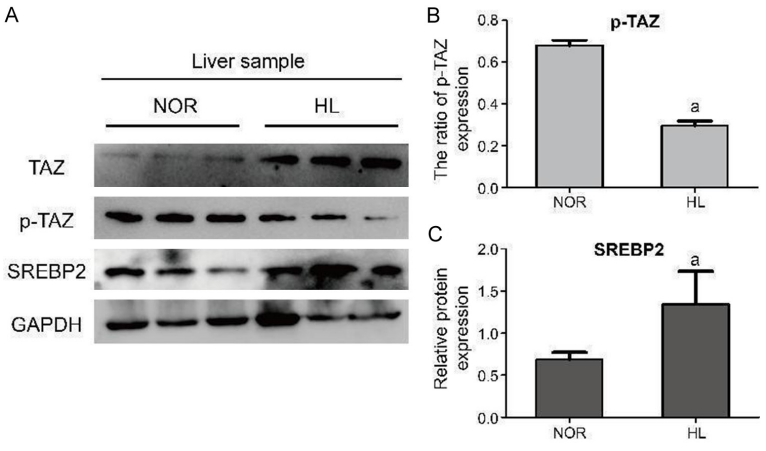

Figure 3. WB analysis between the HL group and the NOR group. A. WB results of the liver sample between the HL group and the NOR group. B. The ratio of p-TAZ expression in total TAZ expression (p-TAZ + TAZ). C. Relative protein expression of SREBP2. $^{a}P < 0.01$, compared with the NOR group. HL group, hepatolithiasis patient group; NOR, normal group; SREBP2, sterol regulatory element-binding protein-2.

lead to severe local biliary issues and are a common cause of mortality associated with benign biliary diseases [35, 36]. The therapeutic principles for managing hepatic bile duct stones include stone removal, alleviating stenosis, ensuring smooth drainage, and preventing recurrence. Research indicates that intrahepatic bile duct exploration and lithotomy, when combined with liver resection, represent a safe and effective approach for treating complex bilateral primary hepatobiliary stones, resulting in satisfactory outcomes [37]. However, there remains a high postoperative

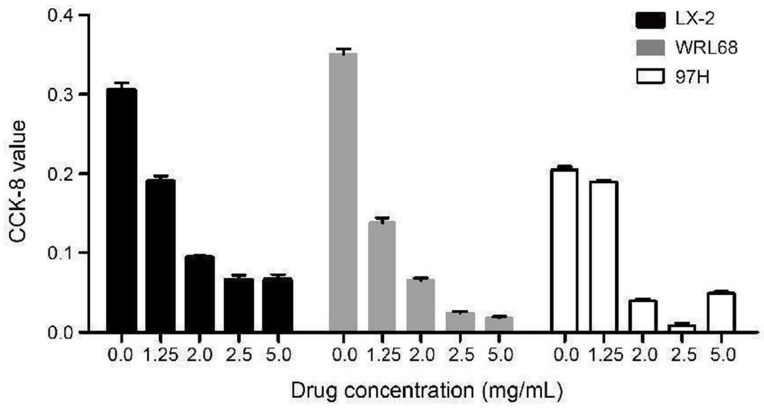

Figure 4. Intervention using TSLG at different drug concentration in cells.

recurrence rate of stones and a significant rate of residual stones, influenced by factors such as bacterial infection and cholestasis [38]. The primary goal of clinical practice is to implement effective preventive measures to reduce the recurrence of stones and enhance patient outcome.

In recent years, the combination of double mirror techniques and the hospital-prepared Twelve Shugan Lidan Granules (TSLG) has shown significant efficacy in the treatment of intrahepatic bile duct stones. Modern pharmacological studies have demonstrated that *Bupleurum* can enhance bile secretion [36], and accelerate bile excretion, significantly improving the dissolution capacity of cholesterol in bile, thereby reducing stone formation. *Curcuma aromatica* is known for its ability to promote qi and alleviate depression, benefit bile, and reduce jaundice [39]. Modern research has demonstrated that Curcuma aromatica offers protective effects on the liver, lowers blood lipids, and possesses antibacterial and anti-inflammatory properties. The active component of Scutellaria baicalensis, baicalin, has been found to effectively inhibit inflammatory responses and protect the liver by preventing carbon tetrachloride-induced damage [40].

Raw rhubarb attack accumulation, wet retreat yellow, has the effect of liver and gallbladder [41]. Studies have shown that *Raw rhubarb* can reduce the serum level of glutamate gamma transaminase, reduce hepatocyte swelling, degeneration and necrosis, and promote liver synthesis capacity and hepatocyte regeneration. *Herba Lysimachiae* is known for its ability to alleviate dampness and reduce jaundice by enhancing bile secretion while simultaneously decreasing total bile acid, free bile acid, and total cholesterol levels in the blood [42]. The combined effects of this prescription can enhance microcirculation in the hepatic bile duct, protect liver enzymes, improve bile flow, and contribute to maintaining homeostasis within the body. This approach minimizes the surgical effect to patients' bodies, improves surgical outcomes, and enhances overall quality of life. Indeed, the results indicate that levels of ALT, AST, and total bilirubin (TB) were significantly reduced in the research group (hepatolithiasis patients administered TSLG postoperatively) compared to the control group (patients without any traditional Chinese medicine treatment). This provides strong experimental evidence for the hepatoprotective effects of TSLG.

To gain a deeper understanding of the pathogenesis of hepatolithiasis (HL) and the efficacy of TSLG, we conducted high-throughput sequencing (HTS) to analyze miRNA expressions in five HL patients and five hepatic hemangioma (HH) patients, with the latter serving as a control group due to their nearly normal liver function (without HL or cirrhosis). The HTS data revealed that 64 miRNAs were differentially expressed in HL patients ($P < 0.05$, fold change ≥ 1), comprising 40 up-regulated and 24 down-regulated miRNAs. Additionally, we performed Gene Ontology (GO) and Kyoto Encyclopedia of Genes and Genomes (KEGG) functional enrichment analyses, which highlighted the abnormal activation of the Hippo signaling pathway in the HL group. This finding was further validated by western blot (WB) testing. The activation of the Hippo signaling pathway in HL patients suggests a link to stone formation. This pathway is a crucial regulator of cell proliferation and apoptosis, with its central components including the tumor suppressor kinases MST1, MST2, LATS1, and LATS2, along with the adaptor proteins SAV1 and MOB1/2 [43-45]. These conserved kinase cassettes inhibit tissue growth (organ size) and progenitor cell proliferation by phosphorylating and inacti-

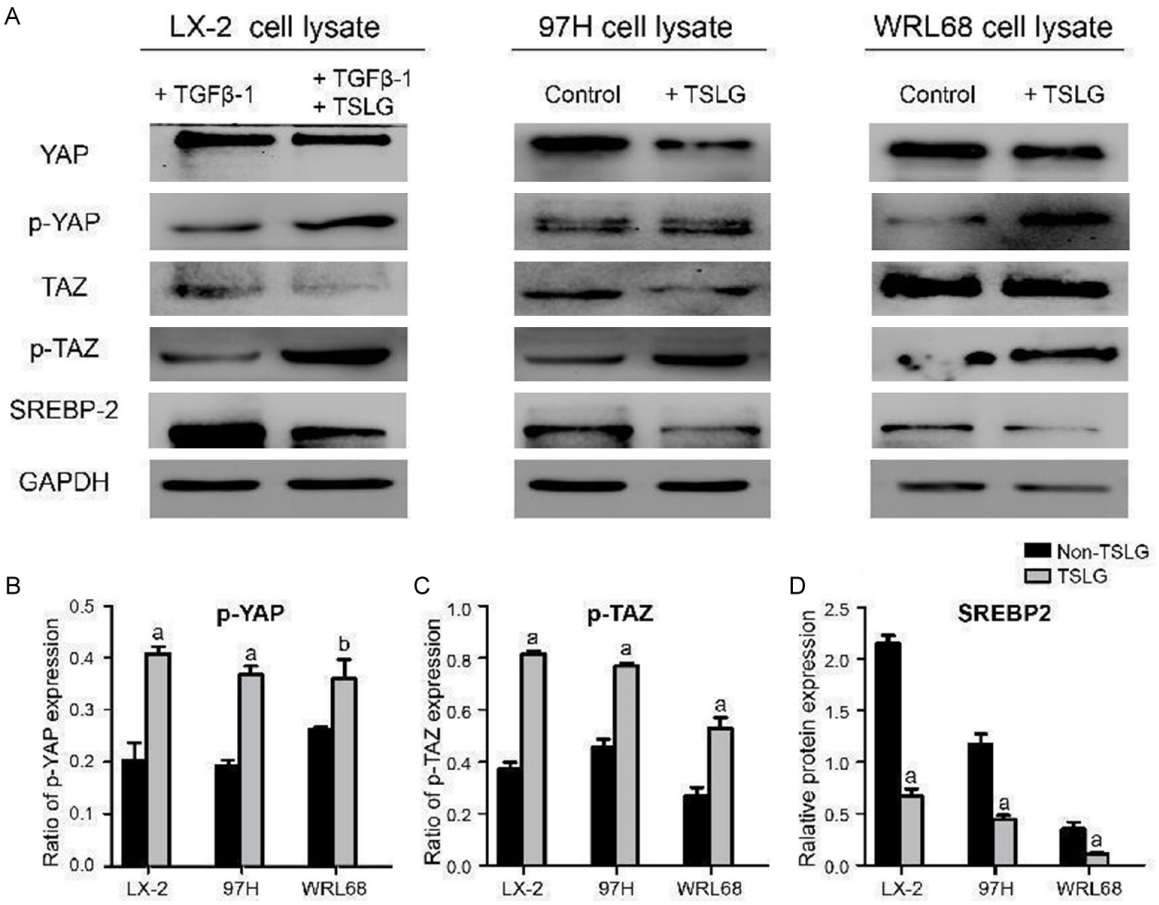

Figure 5. Cell line studies to detect different protein expressions after the intervention of TGFβ-1 and TSLG in LX-2, MHCC97-H and WRL68 cells. A. The WB results for different cell lines. B. The ratio of p-YAP expression in total YAP expression (p-YAP + YAP). C. The ratio of p-TAZ expression in total TAZ expression (p-TAZ + TAZ). D. Relative protein expression of SREBP2. $^{a}P < 0.01$, compared with the non-TSLG group. $^{b}P < 0.05$, compared with the non-TSLG group. SREBP2, sterol regulatory element-binding protein-2.

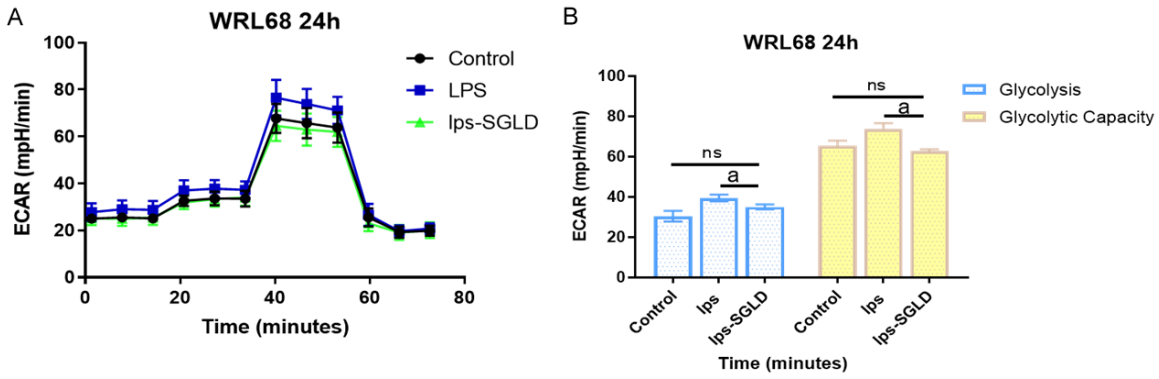

Figure 6. Effect of TSLG on glycolysis after LPS induction of WRL68. A. SeahorseXF measures the ECAR values of cells from three different groups at various time points. B. Quantification of ECAR values of cells from three groups under emergency conditions. $^{a}P < 0.01$ compared with the LPS-induced group. $P > 0.05$, compared with the Control group. ECAR, Extracellular Acidification Rate; ns, not significant.

vating the transcriptional coactivators YAP and TAZ. Notably, LATS2 can bind to the endoplasmic reticulum (ER)-tethered precursors of SREBP1 and SREBP2 (P-SREBP), thereby limit-

ing their transcriptional and biologic activities. The SREBPs (sterol regulatory element-binding proteins), particularly SREBP1 and SREBP2, play a crucial role in regulating cholesterol and lipid metabolism [46-51]. In particular, SREBP1 primarily regulates lipogenic processes, while SREBP2 mainly activates genes related to cholesterol synthesis. Additionally, the downstream effectors YAP and TAZ have been reported to promote cancer through their reliance on the activity of cholesterol and the SREBP-mevalonate pathway. As a signaling hub for metabolism and proliferation, the activities of SREBPs must be finely tuned by Hippo and other cellular pathways. Our cell line studies revealed that protein expression of SREBP2 is significantly downregulated following TSLG intervention, suggesting that TSLG suppresses the Hippo signaling pathway. Further investigation showed that the LPS-induced inflammation model increased both glycolysis and glycolytic capacity in hepatocytes, but these effects were inhibited by TSLG intervention. This finding corroborates our previous results regarding the pathway intervention. Collectively, we propose that the aberrant activation of the Hippo signaling pathway in HL patients disrupts the activities of LAST2 and YAP/TAZ, thereby disturbing the lipid and cholesterol metabolic balance regulated by SREBPs, which may ultimately lead to the formation of intrahepatic bile duct calculi.

Conclusion

Our study evaluated the clinical efficacy of Twelve Shugan Lidan Granules (TSLG), in the treatment of patients with hepatolithiasis. The results demonstrated that TSLG exerts a hepatoprotective effect by improving liver function post-surgery. Omics analysis revealed abnormal activation of the Hippo signaling pathway in HL patients. The underlying mechanism for the clinical efficacy of TSLG in treating HL appears to be associated with the downregulation of SREBP2 and the inhibition of the Hippo signaling pathway, which may help prevent the formation of intrahepatic bile duct calculi.

Acknowledgements

We thank our alma mater Anhui University of Traditional Chinese Medicine for the experimental platform provided for this study. Thank you all for your support and help. This work was supported by the 12th Five-Year national key clinical specialist construction project ([2013] 239).

Disclosure of conflict of interest

None.

Abbreviations

HL, Hepatolithiasis; TSLG, Twelve Shugan Lidan Granules; WB, Western blot; HTS, high-throughput sequencing; ECAR, Extracellular Acidification Rate; SREBP2, sterol regulatory element-binding protein-2; HH, hepatic hemangioma; ALT, alanine aminotransferase; AST, aspartate aminotransferase; TB, total bilirubin; ALB, albumin; NOR, normal group; RT-PCR, reverse transcription-polymerase chain reaction; CPM, counts per million; GO, Gene Ontology; KEGG, Kyoto Encyclopedia of Genes and Genomes; FDR, false discovery rate; SD, standard deviation; BP, biological processes; CC, cellular components; MF, molecular functions; UDC, ursodeoxycholate.

Address correspondence to: Qingsheng Yu and Hui Peng, Department of General Surgery, The First Affiliated Hospital of Anhui University of Chinese Medicine, Hefei 230031, Anhui, P. R. China. Tel: +86-13866141906; E-mail: qsy6312@163.com (QSY); Tel: +86-15155916472; E-mail: ph13638-2333@126.com (HP); Qiyu Feng, Cancer Research Center, The First Affiliated Hospital of USTC, Division of Life Sciences and Medicine, University of Science and Technology of China, Hefei 230036, Anhui, P. R. China. Tel: +86-0551-63607040; E-mail: qiyu@icloud.com

References

[1] Nakayama F and Koga A. Hepatolithiasis: present status. World J Surg 1984; 8: 9-14.
[2] Uchiyama K, Onishi H, Tani M, Kinoshita H, Ueno M and Yamaue H. Indication and procedure for treatment of hepatolithiasis. Arch Surg 2002; 137: 149-153.
[3] Shoda J, Tanaka N and Osuga T. Hepatolithiasis--epidemiology and pathogenesis update. Front Biosci 2003; 8: e398-e409.
[4] Vetrone G, Ercolani G, Grazi GL, Ramacciato G, Ravaioli M, Cescon M, Varotti G, Del Gaudio M, Quintini C and Pinna AD. Surgical therapy for hepatolithiasis: a Western experience. J Am Coll Surg 2006; 202: 306-312.

[5] Lorio E, Patel P, Rosenkranz L, Patel S and Sayana H. Management of hepatolithiasis: review of the literature. Curr Gastroenterol Rep 2020; 22: 30.
[6] Sakpal SV, Babel N and Chamberlain RS. Surgical management of hepatolithiasis. HPB (Oxford) 2009; 11: 194-202.
[7] Nakayama F, Soloway RD, Nakama T, Miyazaki K, Ichimiya H, Sheen PC, Ker CG, Ong GB, Choi TK and Boey J. Hepatolithiasis in East Asia. Retrospective study. Dig Dis Sci 1986; 31: 21-26.
[8] Nakayama F, Koga A, Ichimiya H, Todo S, Shen K, Guo RX, Zeng XJ and Zhang ZH. Hepatolithiasis in East Asia: comparison between Japan and China. J Gastroenterol Hepatol 1991; 6: 155-158.
[9] Yang T, Lau WY, Lai EC, Yang LQ, Zhang J, Yang GS, Lu JH and Wu MC. Hepatectomy for bilateral primary hepatolithiasis: a cohort study. Ann Surg 2010; 251: 84-90.
[10] Kim HJ, Kim JS, Joo MK, Lee BJ, Kim JH, Yeon JE, Park JJ, Byun KS and Bak YT. Hepatolithiasis and intrahepatic cholangiocarcinoma: a review. World J Gastroenterol 2015; 21: 13418-13431.
[11] Tabata M and Nakayama F. Bacteriology of hepatolithiasis. Prog Clin Biol Res 1984; 152: 163-174.
[12] Chen DW, Tung-Ping Poon R, Liu CL, Fan ST and Wong J. Immediate and long-term outcomes of hepatectomy for hepatolithiasis. Surgery 2004; 135: 386-393.
[13] Lee TY, Chen YL, Chang HC, Chan CP and Kuo SJ. Outcomes of hepatectomy for hepatolithiasis. World J Surg 2007; 31: 479-482.
[14] Otani K, Shimizu S, Chijiiwa K, Ogawa T, Morisaki T, Sugitani A, Yamaguchi K and Tanaka M. Comparison of treatments for hepatolithiasis: hepatic resection versus cholangioscopic lithotomy. J Am Coll Surg 1999; 189: 177-182.
[15] Tan J, Tan Y, Chen F, Zhu Y, Leng J and Dong J. Endoscopic or laparoscopic approach for hepatolithiasis in the era of endoscopy in China. Surg Endosc 2015; 29: 154-162.
[16] Su CH, Shyr YM, Lui WY and P'Eng FK. Hepatolithiasis associated with cholangiocarcinoma. Br J Surg 1997; 84: 969-973.
[17] Chen MF, Jan YY, Wang CS, Hwang TL, Jeng LB, Chen SC and Chen TJ. A reappraisal of cholangiocarcinoma in patient with hepatolithiasis. Cancer 1993; 71: 2461-2465.
[18] Chen Q, Zhang Y, Li S, Chen S, Lin X, Li C and Asakawa T. Mechanisms underlying the prevention and treatment of cholelithiasis using traditional Chinese medicine. Evid Based Complement Alternat Med 2019; 2019: 2536452.
[19] Jan YY, Chen MF, Wang CS, Jeng LB, Hwang TL and Chen SC. Surgical treatment of hepatolithiasis: long-term results. Surgery 1996; 120: 509-514.
[20] Fan N, Meng K, Zhang Y, Hu Y, Li D, Gao Q, Wang J, Li Y, Wu S and Cui Y. The effect of ursodeoxycholic acid on the relative expression of the lipid metabolism genes in mouse cholesterol gallstone models. Lipids Health Dis 2020; 19: 158.
[21] Ma Z, Zhang B, Fan Y, Wang M, Kebebe D, Li J and Liu Z. Traditional Chinese medicine combined with hepatic targeted drug delivery systems: a new strategy for the treatment of liver diseases. Biomed Pharmacother 2019; 117: 109128.
[22] Liang Z, Chen X, Shi J, Hu H, Xue Y and Ung COL. Efficacy and safety of traditional Chinese medicines for non-alcoholic fatty liver disease: a systematic literature review of randomized controlled trials. Chin Med 2021; 16: 9.
[23] Liao X, Bu Y and Jia Q. Traditional Chinese medicine as supportive care for the management of liver cancer: past, present, and future. Genes Dis 2019; 7: 370-379.
[24] Han W, Li H, Jiang H, Xu H, Lin Y, Chen J, Bi C and Liu Z. Progress in the mechanism of autophagy and traditional Chinese medicine herb involved in alcohol-related liver disease. PeerJ 2023; 11: e15977.
[25] Zhao CQ, Zhou Y, Ping J and Xu LM. Traditional Chinese medicine for treatment of liver diseases: progress, challenges and opportunities. J Integr Med 2014; 12: 401-408.
[26] Zhang JZ, Zhang XI, Liang XQ, Gu HG and Zhu Pt. Effects of different Chinese herbal medicines on biochemical parameters in guinea-pig with pigment gallstones. Zhong Xi Yi Jie He Xue Bao 2008; 6: 856-859.
[27] Wu Y, Liu L, Zhao Y and Zhao R. Polysaccharides of vinegar-baked radix bupleuri promote the hepatic targeting effect of oxymatrine by regulating the protein expression of HNF4α, Mrp2, and OCT1. J Ethnopharmacol 2021; 267: 113471.
[28] Wang YX, Du Y, Liu XF, Yang FX, Wu X, Tan L, Lu YH, Zhang JW, Zhou F and Wang GJ. A hepatoprotection study of Radix Bupleuri on acetaminophen-induced liver injury based on CYP450 inhibition. Chin J Nat Med 2019; 17: 517-524.
[29] Zhang Q, Zhang L, Liu K, Shang H, Ruan J, Yu Z, Meng S, Liang F, Wang T, Zhang H, Peng W, Wang Y, Chen J, Xiao T and Wang B. A network pharmacology study on the active components and targets of the radix ginseng and radix bupleuri herb pair for treating nonalcoholic fatty liver disease. Evid Based Complement Alternat Med 2022; 2022: 1638740.
[30] Dehzad MJ, Ghalandari H, Amini MR and Askarpour M. Effects of curcumin/turmeric

supplementation on liver function in adults: a GRADE-assessed systematic review and dose-response meta-analysis of randomized controlled trials. Complement Ther Med 2023; 74: 102952.
[31] Abd El-Hack ME, El-Saadony MT, Swelum AA, Arif M, Abo Ghanima MM, Shukry M, Noreldin A, Taha AE and El-Tarabily KA. Curcumin, the active substance of turmeric: its effects on health and ways to improve its bioavailability. J Sci Food Agric 2021; 101: 5747-5762.
[32] Luber RP, Rentsch C, Lontos S, Pope JD, Aung AK, Schneider HG, Kemp W, Roberts SK and Majeed A. Turmeric induced liver injury: a report of two cases. Case Reports Hepatol 2019; 2019: 6741213.
[33] Li R, Guo W, Fu Z, Ding G, Zou Y and Wang Z. Hepatoprotective action of Radix Paeoniae Rubra aqueous extract against CCl4-induced hepatic damage. Molecules 2011; 16: 8684-8694.
[34] Tan YQ, Chen HW, Li J and Wu QJ. Efficacy, chemical constituents, and pharmacological actions of radix paeoniae rubra and radix paeoniae alba. Front Pharmacol 2020; 11: 1054.
[35] Nagappan A, Kim JH, Jung DY and Jung MH. Cryptotanshinone from the salvia miltiorrhiza bunge attenuates ethanol-induced liver injury by activation of AMPK/SIRT1 and Nrf2 signaling pathways. Int J Mol Sci 2019; 21: 265.
[36] Kim CL, Choi SH and Mo JS. Role of the hippo pathway in fibrosis and cancer. Cells 2019; 8: 468.
[37] Zhang J, Lyu Z, Li B, You Z, Cui N, Li Y, Li Y, Huang B, Chen R, Chen Y, Peng Y, Fang J, Wang Q, Miao Q, Tang R, Gershwin ME, Lian M, Xiao X and Ma X. P4HA2 induces hepatic ductular reaction and biliary fibrosis in chronic cholestatic liver diseases. Hepatology 2023; 78: 10-25.
[38] Zheng Y and Pan D. The hippo signaling pathway in development and disease. Dev Cell 2019; 50: 264-282.
[39] Lammert F, Gurusamy K, Ko CW, Miquel JF, Méndez-Sánchez N, Portincasa P, van Erpecum KJ, van Laarhoven CJ and Wang DQ. Gallstones. Nat Rev Dis Primers 2016; 2: 16024.
[40] Chen G, Wu J, Xiao L, Wen Y, Yang T and Wang S. Right posteroinferior bile duct angulation correlates with bile duct stone occurrence in patients with hepatolithiasis. Abdom Radiol (NY) 2020; 45: 3103-3108.
[41] Tazuma S. Gallstone disease: Epidemiology, pathogenesis, and classification of biliary stones (common bile duct and intrahepatic). Best Pract Res Clin Gastroenterol 2006; 20: 1075-1083.
[42] Manti M, Shah J, Papaefthymiou A, Facciorusso A, Ramai D, Tziatzios G, Papadopoulos V, Paraskeva K, Papanikolaou IS, Triantafyllou K, Arvanitakis M, Archibugi L, Vanella G, Hollenbach M and Gkolfakis P. Endoscopic management of difficult biliary stones: an evergreen issue. Medicina (Kaunas) 2024; 60: 340.
[43] Li EL, Yuan RF, Liao WJ, Feng Q, Lei J, Yin XB, Wu LQ and Shao JH. Intrahepatic bile duct exploration lithotomy is a useful adjunctive hepatectomy method for bilateral primary hepatolithiasis: an eight-year experience at a single centre. BMC Surg 2019; 19: 16.
[44] Xia H, Zhang H, Xin X, Liang B, Yang T, Liu Y, Wang J and Meng X. Surgical management of recurrence of primary intrahepatic bile duct stones. Can J Gastroenterol Hepatol 2023; 2023: 5158580.
[45] Sun P, Li Y, Wei S, Zhao T, Wang Y, Song C, Xue L, Wang F, Xiao L, Wu J and Qiao M. Pharmacological effects and chemical constituents of bupleurum. Mini Rev Med Chem 2019; 19: 34-55.
[46] Kim H, Hong J, Lee J, Jeon W, Yeo C, Lee Y, Baek S and Ha I. Curcuma aromatica Salisb. protects from acetaminophen-induced hepatotoxicity by regulating the Sirt1/HO-1 signaling pathway. Nutrients 2023; 15: 808.
[47] Soleimani V, Sahebkar A and Hosseinzadeh H. Turmeric (Curcuma longa) and its major constituent (curcumin) as nontoxic and safe substances: review. Phytother Res 2018; 32: 985-995.
[48] Wang T, Lu Z, Qu XH, Xiong ZY, Wu YT, Luo Y, Zhang ZY, Han XJ and Xie CF. Chrysophanol-8-O-glucoside protects mice against acute liver injury by inhibiting autophagy in hepatic stellate cells and inflammatory response in liver-resident macrophages. Front Pharmacol 2022; 13: 951521.
[49] Jeong YH, Kim TI, Oh YC and Ma JY. Lysimachiae herba inhibits inflammatory reactions and improves lipopolysaccharide/D-Galactosamine-induced hepatic injury. Antioxidants (Basel) 2021; 10: 1387.
[50] Shu Z, Gao Y, Zhang G, Zhou Y, Cao J, Wan D, Zhu X and Xiong W. A functional interaction between Hippo-YAP signalling and SREBPs mediates hepatic steatosis in diabetic mice. J Cell Mol Med 2019; 23: 3616-3628.
[51] Aylon Y and Oren M. The Hippo pathway, p53 and cholesterol. Cell Cycle 2016; 15: 2248-2255.